THE JOURNAL OF PHYSICAL CHEMISTRY A

pubs.acs.org/JPCA Article

S_N2 Reactions of N_2O_5 with Ions in Water: Microscopic Mechanisms, Intermediates, and Products

Natalia V. Karimova, James Chen, Joseph R. Gord, Sean Staudt, Timothy H. Bertram, Gilbert M. Nathanson, and R. Benny Gerber*

Cite This: *J. Phys. Chem. A* 2020, 124, 711−720

Read Online

ACCESS | Metrics & More | Article Recommendations

ABSTRACT: Reactions of dinitrogen pentoxide (N_2O_5) greatly affect the concentrations of NO_3, ozone, OH radicals, methane, and more. In this work, we employ ab initio molecular dynamics and other tools of computational chemistry to explore reactions of N_2O_5 with anions hydrated by 12 water molecules to shed light on this important class of reactions. The ions investigated are Cl^-, SO_4^{2-}, ClO_4^-, and $RCOO^-$ (R = H, CH_3, C_2H_5). The following main results are obtained: (i) all the reactions take place by an S_N2-type mechanism, with a transition state that involves a contact ion pair ($NO_2^+NO_3^-$) that interacts strongly with water molecules. (ii) Reactions of a solvent-separated nitronium ion (NO_2^+) are not observed in any of the cases. (iii) An explanation is provided for the suppression of $ClNO_2$ formation from N_2O_5 reacting with salty water when sulfate or acetate ions are present, as found in recent experiments. (iv) Formation of novel intermediate species, such as ($SO_4NO_2^-$) and $RCOONO_2$, in these reactions is predicted. The results suggest atomistic-level mechanisms for the reactions studied and may be useful for the development of improved modeling of reaction kinetics in aerosol particles.

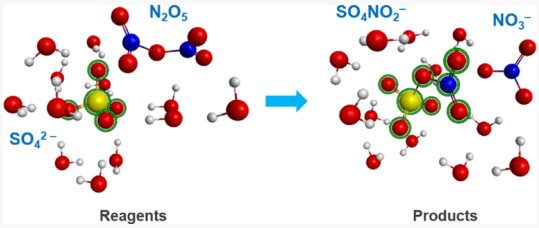

1. INTRODUCTION

Heterogeneous chemical reactions at atmospheric aqueous interfaces between gas-phase molecules and the liquid-phase molecules play a key role in air quality and climate.[1−3] An important example is the reaction of N_2O_5 at the surface of aerosol particles. These reactions affect concentrations of ozone, hydroxyl radicals, methane, and other atmospheric species.[4−10] The molecule N_2O_5 is thermally and photochemically unstable, and formed by recombination of NO_3 and NO_2.[9,11,12] Two of the most atmospherically important processes where N_2O_5 is involved are hydrolysis[13−15] and halide substitution[8,15−17] reactions.

Hydrolysis of dinitrogen pentoxide is believed to occur through the cleavage into ions (NO_2^+)(NO_3^-) of dinitrogen pentoxide in solution, followed by a reaction with water to produce two molecules of nitric acid (HNO_3).[13−15] It was shown that heterogeneous hydrolysis of N_2O_5 in the liquid phase (aqueous aerosols, fog, or cloud droplets) is much faster than homogeneous hydrolysis in the gas phase.[18−20] Heterogeneous hydrolysis is considered to be the dominant pathway for direct chemical loss of atmospheric N_2O_5. In the literature, two mechanisms for hydrolysis of dinitrogen pentoxide are proposed: (i) N_2O_5 molecules are adsorbed at the surface of water, diffuse into the bulk, and then react with water molecules to produce nitric acid molecules[21] and (ii) N_2O_5 reacts with water molecules at the water surface region without diffusion into the bulk.[13,22,23] Additionally, a theoretical study of hydrolysis of N_2O_5 molecules in small water clusters (five water molecules) was performed by Hillier and co-workers.[24] The results showed that the reaction mechanism seems to occur by an S_N2 type of attack of H_2O at a partially positively charged nitrogen atom of the strongly polarized N_2O_5, which is followed by proton transfer to an adjacent water molecule.

It is known that if anions are present in water, the product branching fractions are changed.[11,15,17,25−36] One of the most studied halide substitution reactions is the reaction of N_2O_5 with chloride-containing salty water, causing the formation of nitryl chloride ($ClNO_2$), a source of reactive chlorine radicals in the atmosphere.[8,15−17,25] $ClNO_2$ is formed during the night and undergoes photolysis in the morning to produce halide radicals and nitrogen dioxide (NO_2). Despite the importance of this process, the mechanism of formation of $ClNO_2$ from the reaction between intact N_2O_5 and Cl^- is not completely understood. For example, it is not known whether a transient nitronium ion (NO_2^+)[4,37] is formed prior to the reaction because of dissociation of N_2O_5, or if the formation of $ClNO_2$

Received: September 26, 2019
Revised: December 24, 2019
Published: December 27, 2019

occurs because of the direct reaction between intact N_2O_5 and Cl^-.

To better understand the competition between reactions of N_2O_5 and key anions at the air−seawater interface, theoretical investigations of the potential energy surface and dynamics can be performed using ab initio methods, as seen in related recent studies.[10,24,38−40] For example, the reactions between N_2O_5 and halide ions in the presence of one water molecule were recently studied using molecular dynamics simulations.[38,39] Inspection of the detailed geometries along the trajectories strongly suggests that the mechanism is of the S_N2 type: as the N_2O_5 approaches the halide ion, the NO_3^- group is removed from the NO_2^+ fragment, and a resulting nitryl halide molecule is formed.[39] However, the effects of additional water molecules on the barriers, structures, and mechanisms of N_2O_5 and Cl^- reactions are still unknown.

An additional interesting fact about the $ClNO_2$ yield should be mentioned: determinations of the $ClNO_2$ yield based on field measurements are routinely lower than that predicted based on a chemical mechanism involving only sodium chloride and water solutions.[41−46] This disagreement suggests that the mechanism of $ClNO_2$ production is not completely understood and may be complicated by the presence of additional aerosol components or loss processes that consume $ClNO_2$. A recent experimental study by Staudt et al.[47] reported measurements of the nitryl chloride ($ClNO_2$) branching fraction following reactive uptake of N_2O_5 by mixed organic and inorganic solutions representative of atmospheric interfaces. Different ions present in seawater were considered in that work: (i) the sulfate ion (SO_4^{2-}), because it is one of the most abundant ions in seawater aerosols and may play a significant role in halogen activation in the atmosphere. (ii) The perchlorate ion (ClO_4^-). This ion is a water-soluble species, with concentrations in seawater in the range of <0.07 to 0.34 μg/L. Perchlorate has both natural and anthropogenic occurrences in water all over the world. (iii) Carboxylic acid anions ($RCOO^-$). These anions are ubiquitous in aerosols and in other atmospheric systems.[48] The results of Staudt et al.[47] show that sulfate and acetate ions reduce the branching fraction of the $ClNO_2$ product in the reaction of N_2O_5 in water containing, whereas no statistically significant suppression of the Cl^- yield was observed in the presence of the perchlorate ion. This study indicates that anions that are ubiquitous in atmospheric aerosols, yet commonly believed to be nonreactive, may regulate the production of reactive gases such as $ClNO_2$. In addition, important information about macroscopic parameters of the formation process of $ClNO_2$ in the atmosphere was obtained. However, the microscopic mechanisms of the reactions of N_2O_5 with sulfate, perchlorate, and carboxylic ions have not yet been unraveled.

In this work, we aim to understand the mechanisms of chemical reactions of N_2O_5 with hydrated inorganic and organic ions [Cl^-, SO_4^{2-}, ClO_4^-, and $RCOO^-$ (R = H, CH_3, C_2H_5)] using ab initio quantum-chemical methods such as the calculations of potential energy surfaces (PESs), determinations of transition states (TSs), and ab initio molecular dynamics (AIMD) simulations. The results are in good agreement with the above-noted experimental findings[47] and provide an interpretation of the suppression of $ClNO_2$ formation when N_2O_5 reacts with salty water when sulfate or acetate ions are present. Additionally, the formation of novel intermediate species or products, such as ($SO_4NO_2^-$) and $RCOONO_2$, in the reactions is predicted.

2. COMPUTATIONAL DETAILS

In this study, the reactions of N_2O_5 with Cl^-, SO_4^{2-}, ClO_4^-, and $RCOO^-$ (R = H, CH_3, C_2H_5) at the air−water interface are studied and the competition of these reactions (R1−R5) is considered with respect to the experimental study performed by Staudt et al.[47] The first four reactions involve reactions of N_2O_5 with hydrated anions (R1−R4), whereas the last process (R5) is a case when $ClNO_2$ molecules are attacked and transformed by sulfate ions. This last reaction has the potential to impact the $ClNO_2$ concentrations in the atmosphere and/or the interpretation of experiments on the $ClNO_2$ branching fraction.

$$(Cl^-) + N_2O_5 \rightarrow ClNO_2 + (NO_3^-) \quad \text{(R1)}$$

$$(SO_4^{2-}) + N_2O_5 \rightarrow (SO_4NO_2^-) + (NO_3^-) \quad \text{(R2)}$$

$$(RCOO^-) + N_2O_5 \rightarrow RCOONO_2 + (NO_3^-) \quad \text{(R3)}$$

$$(ClO_4^-) + N_2O_5 \rightarrow ClO_4NO_2 + (NO_3^-) \quad \text{(R4)}$$

$$(SO_4^{2-}) + ClNO_2 \rightarrow (SO_4NO_2^-) + (Cl^-) \quad \text{(R5)}$$

To understand these processes, it is necessary to develop simplified theoretical models to describe the correct reaction mechanism at a reasonable computational cost. In order to choose the minimum number of water molecules in our models, we need to understand the preferable location of these ions in water media. It is well known that the one of the largest ions considered, the sulfate ion, tends to be fully solvated.[49−51] Recent theoretical results show that SO_4^{2-} requires 12 water molecules to complete the first solvent shell.[49−51] Therefore, we need to include at least 12 water molecules in our models to stabilize the sulfate ion. Because SO_4^{2-} requires 12 water molecules, the same number of water molecules were chosen for all systems considered for consistency. The model systems used are $(N_2O_5)(X)(H_2O)_{12}$ where X = Cl^-, SO_4^{2-}, ClO_4^-, and $HCOO^-$. It should be noted that our suggested model is applicable for studying the elementary chemical reactions, but it cannot describe the role of diffusion[47] that certainly influences the kinetics in the macroscopic system.

Determination of the initial structures of the hydrated ions $(X)(H_2O)_{12}$ (where X = Cl^-, SO_4^{2-}, ClO_4^-, and $HCOO^-$) is an important step of this work. The global minimum structures of $(SO_4^{2-})(H_2O)_{12}$ and $(ClO_4^-)(H_2O)_{12}$ were found in the literature,[49,50] whereas geometries of $(Cl^-)(H_2O)_{12}$ and $(HCOO^-)(H_2O)_{12}$ clusters were determined in this study. To generate possible structures of $(Cl^-)(H_2O)_{12}$ and $(HCOO^-)(H_2O)_{12}$, the Packmol[52] program was used by randomly inserting 12 water molecules and the anion into a sphere of radius 3.5 Å. We generated 150 different initial structures using this program. The clusters were first optimized using the restricted Hartree−Fock method in the 6-31+G* basis set. The most energetically favorable structures were selected for optimization using the density functional theory (DFT) level of theory (PBE0-D/6-31+G*). It should be mentioned that we expect that in the reaction dynamics there will be contributions from all types of structures.

To better understand the role of solvent effects on the reaction of N_2O_5 with anions, models of a smaller size were applied as well (systems with just six water molecules) $(N_2O_5)(X)(H_2O)_6$ were considered (X = Cl^-, SO_4^{2-}, ClO_4^- and $RCOO^-$). These small clusters were used to study the

https://dx.doi.org/10.1021/acs.jpca.9b09095
J. Phys. Chem. A 2020, 124, 711−720

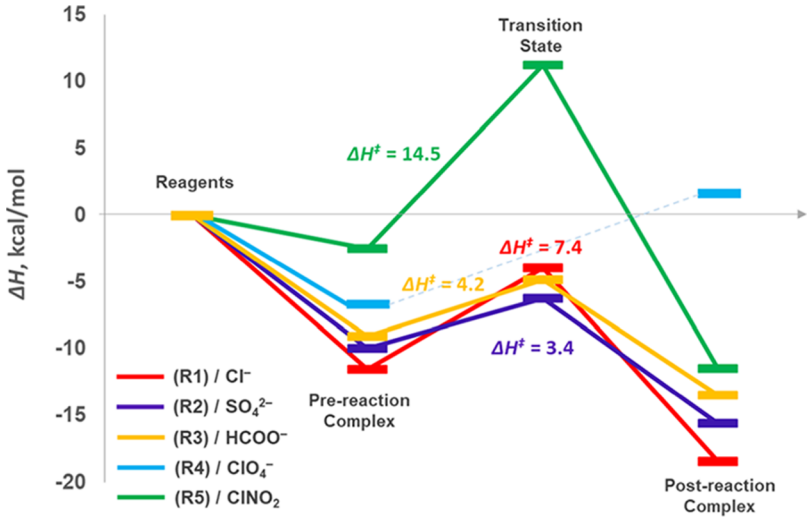

Figure 1. Pathways of (R1−R5) reactions in the gas phase (PBE0-D/6-31+G*). (In the case of reactions (R1−R4) the reagents are N_2O_5 + $(X)(H_2O)_{12}$, whereas for reaction (R5) the reagents are $ClNO_2$ + $(SO_4^{2-})(H_2O)_{12}$). It should be noted that for systems with 12 water molecules, carboxylate ions were modeled with only the formate ion (R3).

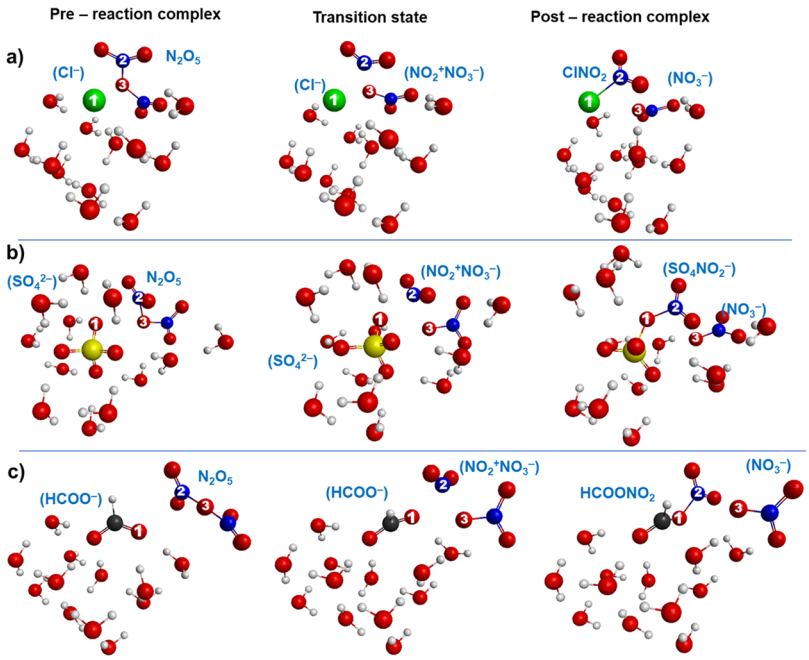

Figure 2. Characteristic structures of the (R1−R3) reactions' profile using (PBE0/6-31+G*): (a) reaction (R1) $(N_2O_5)(Cl^-)(H_2O)_{12} \rightarrow (ClNO_2)(NO_3^-)(H_2O)_{12}$; (b) reaction (R2) $(N_2O_5)(SO_4^{2-})(H_2O)_{12} \rightarrow (SO_4NO_2^-)(NO_3^-)(H_2O)_{12}$; and (c) reaction (R3) $(N_2O_5)(HCOO^-)(H_2O)_{12} \rightarrow (HCOONO_2)(NO_3^-)(H_2O)_{12}$. Atom colors: yellow—sulfur, red—oxygen, blue—nitrogen, and white—hydrogen.

effect of the size of the R-group in the ions of carboxylic acids $RCOO^-$ (R = H, CH_3, C_2H_5).

We combine calculations of PESs, TSs, and AIMD to study the reaction of N_2O_5 molecules with anions. The PESs were initially investigated using DFT with the PBE0 hybrid functional[53] and 6-31+G* basis set using the Q-Chem[54] and GAMESS[55] programs. It has been shown that the PBE0 functional works well for water clusters and ion-water systems.[56,57] Additionally, the DFT-D2 dispersion correction from Grimme is used.[58] In this paper, the abbreviation PBE0-D/6-31+G* is used for this level of theory. The number of negative eigenvalues of the Hessian matrix was examined for all stationary points. Additionally, zero-point energies, enthalpies, and Gibbs free energies (at 298 K) were used for thermochemical analysis. All resulting TSs were linked to their corresponding PES minima by descending along the reaction coordinate using the Gonzalez−Schlegel algorithm (intrinsic reaction coordinate, IRC).[59] The analysis of natural bond orbital (NBO)[60] atomic charges was performed using the PBE0-D/6-31+G* method.

Both "static" free energy calculations and dynamics simulations can certainly contribute to understanding of the reactions of N_2O_5 with different ions. We believe that trajectory simulations in time offer great insights into the mechanism of the processes; for example, how do the partial charges of the atoms change in time from the TS and into product formation. It is not easy to get such insights from static simulations. To explore the reaction mechanisms at 298 K

https://dx.doi.org/10.1021/acs.jpca.9b09095
J. Phys. Chem. A 2020, 124, 711−720

Table 1. Geometrical Parameters (Bond Lengths, Å) of the Prereaction Complex, TS, and Post-Reaction Complex of the (R1−R3) Reactions

	prereaction complex $(N_2O_5)(X)(H_2O)_{12}$			TS $(NO_2^+NO_3^-)(X)(H_2O)_{12}$			postreaction complex $[X(NO_2^+)](NO_3^-)(H_2O)_{12}$		
	X = Cl^-	X = SO_4^{2-}	X = $HCOO^-$	X = Cl^-	X = SO_4^{2-}	X = $HCOO^-$	X = Cl^-	X = SO_4^{2-}	X = $HCOO^-$
$R(X^{(1)}N^{(2)})$	3.12	2.57	2.73	2.35	1.96	2.13	1.83	1.42	1.46
$R(N^{(2)}O^{(3)})$[a]	1.52	1.64	1.48	2.07	2.16	1.86	2.78	2.72	2.70

[a]The gas phase value of $R(N^{(2)}O^{(3)})$ is 1.47 Å.

between N_2O_5 and the hydrated ions, we used AIMD[61,62] simulations at constant energy, with potentials at the PBE0-D/6-31+G* level of theory. Two types of initial configurations were used for AIMD simulations (*NVE*): (i) prereaction complexes $(N_2O_5)(X)(H_2O)_6$ (trajectories were carried out for ∼7 ps) and (ii) TS structures with a calculation time of ∼4 ps. Initial velocities were sampled for the equilibrium structure of interest from a Boltzmann distribution at 298 K. Overall, a total of 10 reactive trajectories per system were propagated for up to 7.0 ps using a time-step of 0.4 fs. Additionally, it should be mentioned that the AIMD simulations from the TS[63] can be successfully applied in cases when very-long-time trajectories are required to observe the reactions when initiated at the minimum. AIMD simulations from the TS make it possible to obtain information about reaction pathways and significantly reduce the computational costs.

3. RESULTS

3.1. Reaction Mechanism. The reaction (R1−R5) pathways are presented in Figure 1. All reactions are exothermic (R1−R3 and R5), with the exception of the (R4) reaction of N_2O_5 with the ClO_4^- ion ($\Delta H_{(reaction)}$ = +1.7 kcal/mol and $\Delta G_{(reaction)}$ = +14.6 kcal/mol), making the process of ClO_4NO_2 formation thermodynamically unfavorable at 298 K. This theoretical finding supports the experimental results that the presence of perchlorate ion in chlorine solutions does not affect the yield of $ClNO_2$ in the reactions with N_2O_5.[47] For this reason, only the mechanisms of reactions (R1), (R2), (R3), and (R5) will be considered in this work in detail.

3.1.1. Reaction (R1−R3). N_2O_5 forms stable prereaction complexes $(N_2O_5)(X)(H_2O)_{12}$ with all hydrated ions $(X)(H_2O)_{12}$ (where X = Cl^-, SO_4^{2-}, and $HCOO^-$) (Figure 2a−c). The binding energies of these complexes are 9.1−11.5 kcal/mol and increase in the series $HCOO^- < SO_4^{2-} < Cl^-$ (Figure 1). It should be noted that interaction of N_2O_5 with chloride and formate ions occurs on the surface of the water cluster, whereas in the case of the hydrated sulfate ion, the N_2O_5 molecule successfully penetrates the solvent shell of this ion and attacks it. The formation of the prereaction complex $(N_2O_5)(X)(H_2O)_{12}$ is accompanied by changes in the geometrical parameters of the molecule of N_2O_5. For example, the bond distance between (NO_2^+) and (NO_3^-) fragments increases (with respect to an isolated molecule of N_2O_5 in the gas phase) in the presence of all anions considered. As shown in Table 1 and Figure 2, the most significant changes in this bond length (∼0.17 Å) were found for the sulfate system.

The reaction between N_2O_5 and anions in the complex $(N_2O_5)(X)(H_2O)_{12}$ occurs via a TS $(NO_2^+NO_3^-)(X)(H_2O)_{12}$, where X = Cl^-, SO_4^{2-}, and $HCOO^-$ (Figure 1 and 2). In the TS, the bond length $N^{(2)}O^{(3)}$ between fragments $(NO_2)-(NO_3)$ dramatically increased (by 0.40−0.70 Å with respect to isolated N_2O_5). The longest distance $N^{(2)}O^{(3)}$ is found for the TS of the sulfate system (Table 1). In the systems with sulfate and formate ions, the barriers to the reaction are 3.4 and 4.2 kcal/mol, respectively. The barrier in the system with chloride is substantially larger by 7.4 kcal/mol. As a whole, the activation barrier increases in the order $SO_4^{2-} < HCOO^- < Cl^-$ (Figure 1).

Following the reaction coordinate, the systems turn into $[X(NO_2^+)](NO_3^-)(H_2O)_{12}$ postreaction complexes, where X = Cl^-, SO_4^{2-}, and $HCOO^-$. Calculations show that the interaction of N_2O_5 with chloride ion leads to the formation of $ClNO_2$, for which the enthalpy and free energy of reaction (R1) is found to be ΔH = −19.5 kcal/mol and ΔG = −9.6 kcal/mol (Figure 1). In the case of the reaction of N_2O_5 with sulfate (R2) and carboxylate ions (R3), two novel atmospherically relevant species $(SO_4NO_2^-)$ ion and acetyl nitrate $(HCOONO_2)$ were determined: ΔH = −15.6 kcal/mol (ΔG = −9.1 kcal/mol) and ΔH = −13.5 kcal/mol (ΔG = −2.3 kcal/mol), respectively (Figure 1).

The charge effect of the considered ions can play a key role in determining the ion distribution and the water surface at the gas/liquid interface and as a result affects the reactivity of these ions. Here, we present the analysis of Mulliken atomic charges of ions considered in the prereaction complexes $(N_2O_5)(X)(H_2O)_{12}$ (where X = Cl^-, SO_4^{2-}, and $HCOO^-$). The ions Cl^- and ClO_4^- both are monovalent ions. However, in comparison to Cl^-, which has almost full negative charge localized on this single chlorine atom (charge = −0.80), perchloride ion ClO_4^- is a large tetrahedrally structured system with the negative charge divided between four peripheral oxygen atoms (the average charge on one oxygen atom = −0.53). Hence, the chloride ion is more negative compared with oxygen atoms of the perchlorate ion, which can explain why Cl^- easily reacts with N_2O_5 at 298 K and the nonreactive behavior of ClO_4^-. The sulfate ion is also a large tetrahedral oxyanion, but it has a very large negative charge compared with monovalent ions. Also, the Mulliken atomic charges on the oxygen atoms of the sulfate ion are more negative than for the chloride anion, and the oxygens of ClO_4^-. This can explain the higher reactivity of the sulfate ion with respect to chloride ions in reactions with N_2O_5. In the case of a formate ion, the negative charge is distributed between two oxygen atoms (charges are −0.81 and −0.71). These charge values on oxygen atoms of the $HCOO^-$ ion should make the reactivity of the formate ion similar to that of chloride. However, theoretical and experimental studies showed that carboxylate ions are more effective in reactions with N_2O_5 than chloride. This can be explained by the nature and orientation of nonbonding p-orbitals on oxygen atoms of the $HCOO^-$ ion: attacking the oxygen atom of formate ion has a relatively large nonbonding p-orbital, which is oriented in the direction of the nitrogen atom of the (NO_2^+) fragment in the N_2O_5 molecule. In the case of the chloride ion, the p-orbital does not exhibit this type of orientation.

Additionally, based on the inspection of the geometries of stationary points on PESs, the S_N2 type mechanism is seen to

https://dx.doi.org/10.1021/acs.jpca.9b09095
J. Phys. Chem. A 2020, 124, 711−720

Table 2. NBO Charges of the Prereaction Complex, TS, and Postreaction Complex of the (R1−R3) Reactions (PBE0-D/6-31+G*)

	prereaction complex $(N_2O_5)(X)(H_2O)_{12}$			TS $(NO_2^+NO_3^-)(X)(H_2O)_{12}$			postreaction complex $[X(NO_2^+)](NO_3^-)(H_2O)_{12}$		
	X = Cl^-	X = SO_4^{2-}	X = $HCOO^-$	X = Cl^-	X = SO_4^{2-}	X = $HCOO^-$	X = Cl^-	X = SO_4^{2-}	X = $HCOO^-$
$\delta(X)$	−0.83	−1.72	−0.83	−0.55	−1.49	−0.66	+0.03	−1.00	−0.21
$\delta(NO_2^+)$	+0.21	+0.33	+0.17	+0.31	+0.47	+0.33	−0.03	+0.09	+0.15
$\delta(NO_3^-)$	−0.21	−0.34	−0.17	−0.65	−0.77	−0.54	−0.86	−0.90	−0.88

describe each process: as N_2O_5 approaches the Cl^-, SO_4^{2-}, and $HCOO^-$ ions, the NO_3^- group is separated from the NO_2^+ fragment, and the resulting $ClNO_2$, $SO_4NO_2^-$, and $HCOONO_2$ species are formed. Partial charge analysis fits the S_N2 mechanism as well: (i) in the initial complexes, N_2O_5 is a neutral molecule and substantial negative partial charge is localized on the anion (Table 2). (ii) In the TS, the partial charge of the anion becomes less negative, whereas the N_2O_5 has a strong ion-pair character (Table 2). (iii) In the postreaction complex, the fragment NO_3 is separated from the product $[X(NO_2^+)]$ and exhibits an increase in the negative partial charge closer to −1.

3.1.2. Behavior of the N_2O_5 Molecule in (R1−R3) Reactions. There are two proposed mechanisms for N_2O_5 reactions with anions in the literature.[4] According to the first one, N_2O_5 dissolves in water and dissociates into (NO_3^-) and nitronium ions (NO_2^+) or a hydrated (NO_2^+) intermediate.[13,64,65] In the presence of stronger nucleophiles, such as halide ions, the nitronium ion reacts with them to form nitryl halides XNO_2 (where X = Cl, Br, or I). Another proposed mechanism for the formation of $ClNO_2$ occurs through the formation of an intermediate ion pair $(NO_2^+NO_3^-)$ in the water surface region.[66]

In all our simulations of the reactions N_2O_5 with anions, we did not observe any evidence for formation of the nitronium ion (NO_2^+) as a solvent-separated species. In fact, (NO_2^+) is a strongly coupled part of the $(NO_2^+NO_3^-)$ ion pair, which also is in substantial interaction with at least one water molecule (Figure 2). Even in the TS, we do not see the dissociation of molecular N_2O_5 and separation of the (NO_2^+) and (NO_3^-) fragments (Figure 2, Table 1).

The issue of the nitronium ion in small water clusters was addressed by ab initio calculations.[67] In systems with $n > 3$ water molecules, (NO_2^+) reacts with water molecules to form the nitric acid−hydronium ion−water complex. It should be mentioned that in ref 67, a more nucleophilic group than water was not present. Similar results were obtained for nitrosonium ion, (NO^+).[68] There is no inconsistency between our conclusions and the above study,[67] according to which NO_2^+ cannot exist in the vicinity of more than three water molecules.

In this work, for systems with 12 water molecules, we did not see any evidence of dissociation of N_2O_5 molecules with formation of solvated nitronium ions. The results showed that in the prereaction complex, the bond distance between $NO_2\cdots NO_3$ fragments slightly increases (with respect to an isolated molecule of N_2O_5 in the gas phase) in the presence of anions considered up to 0.17 Å. Only in the TS does this bond-length increase significantly up to 0.70 Å. There is, however, not even a partial penetration of a water molecule, between the $NO_2^{(+\delta)}$ and the $NO_3^{(-\delta)}$. Thus, the N_2O_5 molecule should be considered a contact ion pair $(NO_2^+NO_3^-)$ in the TS region, when the reaction begins.

3.1.3. Solvent Effects and Role of the R-Group. To investigate the role of solvent effects, we considered the reactions of N_2O_5 with hydrated anions with small water clusters $(N_2O_5)(X)(H_2O)_6$ (where X = Cl^-, SO_4^{2-}, $RCOO^-$ and R = H, CH_3, C_2H_5). The results showed that these small models provide reasonable results for systems with surface ions such as chloride and formate ions: reaction of N_2O_5 with $(Cl^-)(H_2O)_6$ has a barrier ∼twice higher than the barrier for reaction with $(HCOO^-)(H_2O)_6$: the barrier the reaction of N_2O_5 with chloride ion is 3.7 kcal/mol, whereas with formate ion it is 2.2 kcal/mol. In the case of sulfate ions, the reaction in the presence of six water molecules occurs without any barrier. These results showed that solvation effects play an important role, especially in the case of sulfate ions. Also, it appears that the size of the R-group of the carboxylate ions does not affect the TS barrier of the reaction N_2O_5 with $RCOO^-$ (where R = H, CH_3, C_2H_5). Barriers of all these reactions are close to ∼2 kcal/mol (range is 2.2−2.5 kcal/mol). Thus, the $HCOO^-$ can be considered as a simple model for simulations of larger carboxylate ions such as CH_3COO^- and $C_2H_5COO^-$.

3.1.4. Reaction (R5). The possible transformation of the $ClNO_2$ molecule during its interaction with a sulfate ion was also considered. $ClNO_2$ forms a relatively stable complex with the hydrated sulfate ion cluster $(ClNO_2)$ $(SO_4^{2-})(H_2O)_{12}$ (Figure 1). Following along the reaction coordinate through the TS leads to the postreaction complex $(Cl^-)(SO_4NO_2^-)$-$(H_2O)_{12}$. However, the barrier of this reaction is 14.5 kcal/mol (Figure 1), implying that sulfate ions will react with N_2O_5 first rather than displacing chloride ions in the $ClNO_2$ molecule.

3.2. AIMD Simulations of the Reaction of N_2O_5 with Hydrated Ions $(X)(H_2O)_{12}$ (where X = Cl^-, SO_4^{2-}, and $HCOO^-$). AIMD simulations (*NVE*) were performed for reactions (R1−R3) from the prereaction complexes (N_2O_5)-$(X)(H_2O)_6$ (where X = Cl^-, SO_4^{2-}, $HCOO^-$). Simulations were carried out for ∼7 ps, but no reaction was observed during this time. Thus, more time is required to observe these reactions in AIMD simulations initiated at the minimum. For this reason, the TS structures were used as the initial configurations in AIMD simulations (with a calculation time of ∼4 ps). From the TS, the system can evolve directly to the products or reagents.

For all ions (chloride, sulfate, and formate ions), 50% of the trajectories are reactive, for example, lead to formation of product $ClNO_2$, $(SO_4NO_2^-)$, and $HCOONO_2$, respectively. The rest of the trajectories are nonreactive and go back directly to the reagent complexes of the hydrated anion and N_2O_5 molecule. Reactive trajectories for all considered anions show similar behavior: as N_2O_5 reacts with the anion, the (NO_3^-) group is separated from the (NO_2^+) moiety, at the same time (NO_2^+) tends to move closer to the anion, and product species such as $ClNO_2$, $SO_4NO_2^-$, and $HCOONO_2$ are formed.

Examples of the reactive and nonreactive trajectories are considered for the sulfate ion system and are presented in

https://dx.doi.org/10.1021/acs.jpca.9b09095
J. Phys. Chem. A 2020, 124, 711−720

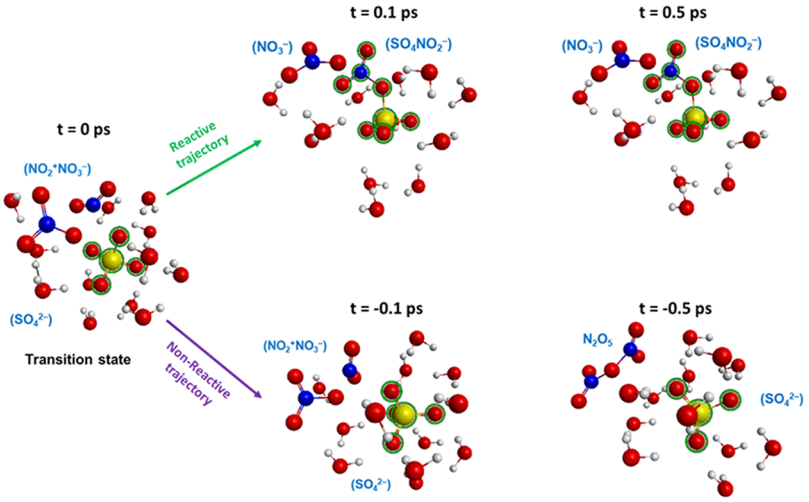

Figure 3. AIMD trajectories configurations (first 0.5 ps) for reaction (R2) N_2O_5 with $(SO_4^{2-})(H_2O)_{12}$. The TS is the initial structure. Atom colors: yellow—sulfur, red—oxygen, blue—nitrogen, and white—hydrogen. Sulfate ions are circled by green.

Figure 3. According to the reactive trajectories, the $SO_4NO_2^-$ product ion is formed in the first 0.1 ps as the distance between NO_2^+ and SO_4^{2-} is shortened and NO_3^- separates from NO_2^+ (Figure 3). Following this 0.1 ps time, the NO_3^- group continues to separate from the product $SO_4NO_2^-$ ion. Nonreactive trajectories exhibit the reformation of N_2O_5 from the TS structure in the first 0.1−0.2 ps.

NBO calculations[60] were performed along both reactive and nonreactive trajectories (Figure 4a−c) in order to examine the partial charges of the Cl, SO_4, HCOO, NO_2, and NO_3 fragments in time. For the sulfate-containing system, the partial charge of the SO_4 group is seen to decrease significantly from ∼−1.75 a.u. in the initial structure to ∼−1 a.u. after product ($SO_4NO_2^-$) formation (Figure 4b). The partial charge on the NO_3 group increases to ∼−1 a.u. after reaction occurs (Figure 4b). The positive partial charge on the NO_2 group falls to ∼0 a.u. throughout the reactive trajectory.

Overall, the trajectories, including analysis of the charges, indicate that the reaction occurs from the TS structure within ∼0.1 ps at room temperature. Inspection of the geometries along the trajectories strongly suggests that the mechanism is of the S_N2 type: during the reaction of N_2O_5 with SO_4^{2-}, the (NO_3^-) fragment moves away from the (NO_2^+) group during the same time that (NO_2^+) moves toward SO_4^{2-} and product ($SO_4NO_2^-$) species is formed. Similar results were obtained for other anions such as chloride and formate ions (Figure 4): product formation is fast and occurs because of attraction between ions in the (X)/(NO_2^+) pairs, where X = Cl^-, SO_4^{2-}, and $HCOO^-$.

3.3. Interpretation of the Experiments of ref 47.

In recent experiments, Staudt et al.[47] reported measurements of the nitryl chloride ($ClNO_2$) branching fraction following reactive uptake of N_2O_5 to mixed organic and inorganic solutions representative of atmospheric interfaces. It was shown that the effect on the $ClNO_2$ branching spanned 0.85 in 0.5 M NaCl to 0.32 in 2.0 M Na_2SO_4 and to 0.18 in 0.5 M NaOAc, but there was no statistically meaningful effect in up to 3.0 M $NaClO_4$. Therefore, both sulfate and carboxylate anions significantly suppress $ClNO_2$ formation from N_2O_5 reacting with chloride-containing solutions. The presence of sodium perchlorate, however, had a much smaller effect on the $ClNO_2$ yield.

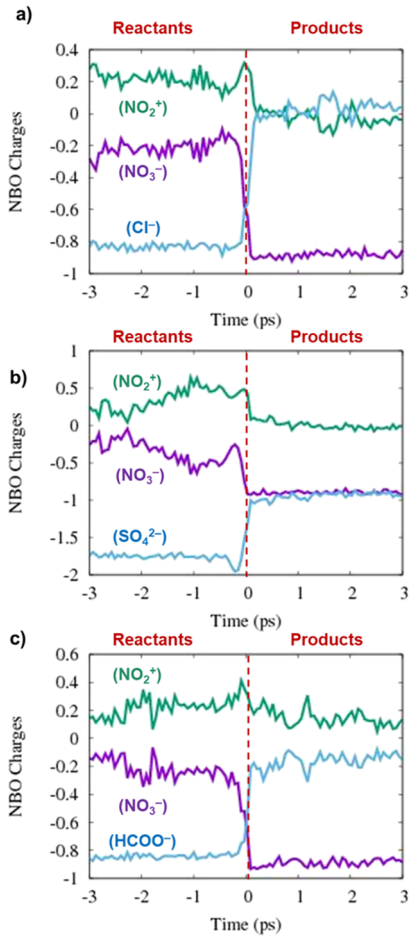

Figure 4. NBO charges along the reactive (0 to 3 ps) and nonreactive (0 to −3 ps) trajectories of reactions: (a) R1, (b) R2, and (c) R3 at 12 water clusters (PBE0-D/6-31+G*).

Our results are in good agreement with these experiments.[47] The reaction of N_2O_5 with the chloride ion has a barrier approximately two times higher than reactions with sulfate and carboxylate ions, which is in accord with the suppression of $ClNO_2$ formation in the presence of sulfate and carboxylate

https://dx.doi.org/10.1021/acs.jpca.9b09095
J. Phys. Chem. A 2020, 124, 711−720

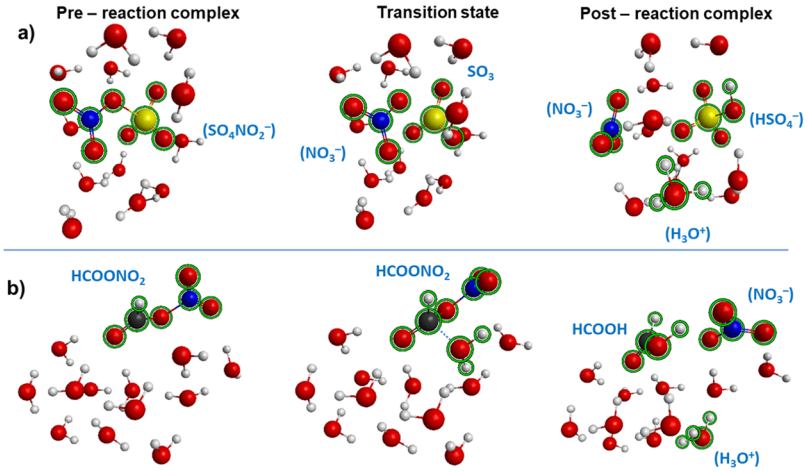

Figure 5. Characteristic structures of the (R6 and R7) reactions' profile (PBE0/6-31+G*). Atom colors: yellow—sulfur, red—oxygen, blue—nitrogen, and white—hydrogen. Ions are circled by green.

ions. The reaction of N_2O_5 with the perchlorate ion is endothermic and cannot affect $ClNO_2$ formation at 289 K.

It is important to mention that the theoretical models we employed to study the reaction mechanisms involve hydrated anions in interaction with N_2O_5, and these models cannot describe the role of diffusion that certainly influences the kinetics[47] in the macroscopic system. However, we believe that these models can be useful for simulations of the chemical reactions themselves and provide a microscopic understanding of reactions.

3.4. Intermediates. Next, we consider the stability of intriguing intermediates such as $SO_4NO_2^-$ and $HCOONO_2$. In this section, we consider their further transformations in the water clusters. One possible route for both species is hydrolysis (R6 and R7)

$$(SO_4NO_2^-) + H_2O \rightarrow (SO_4^{2-}) + (NO_3^-) + 2(H^+) \quad \text{(R6)}$$

$$RCOONO_2 + H_2O \rightarrow (RCOO^-) + (NO_3^-) + 2(H^+) \quad \text{(R7)}$$

When reactions (R6) and (R7) occur, it can be seen that the sulfate and acetate ions play the roles of catalysts in the overall processes. To study these reactions, the calculations of TS and IRC were performed. The initial structures of $(SO_4NO_2^-)$-$(H_2O)_{12}$ and $(HCOONO_2)(H_2O)_{12}$ are presented in Figure 5. The $(SO_4NO_2^-)$ is fully solvated and located in the center of the water cluster, whereas the $HCOONO_2$ species is considered on the surface of the $(H_2O)_{12}$.

The pathways for the hydrolysis of these two species in the water clusters are different (Figure 5). Our results show that reaction (R6) requires the dissociation of $(SO_4NO_2^-)$ into (NO_3^-) and SO_3 fragments in the TS, after which water attacks SO_3 to form (HSO_4^-) and (H_3O^+) ions (Figure 5a). The barrier for this reaction is less than 1 kcal/mol.

In the case of reaction (R7), one of the water molecules directly attacks the carbon center of $HCOONO_2$ and forms the $(H_2O\cdots HCOONO_2)(H_2O)_{11}$ TS (with a barrier of 7.4 kcal/mol). Following the reaction coordinate, the TS $(H_2O\cdots HCOONO_2)(H_2O)_{11}$ turns into HCOOH, (H_3O^+), and (NO_3^-) fragments via proton transfer and separation of NO_3 group, which are found to be barrierless processes and occur spontaneously.

4. CONCLUSIONS

The atmospherically important class of reactions of anions in water with N_2O_5 was explored computationally by methods that include AIMD and TS calculations. The models used were hydrated anions in $n = 12$ water clusters. Whereas this model does not address aspects such as diffusion of ions in the corresponding macroscopic systems, we believe that it realistically describes the chemical reaction itself. Several anions were studied using this framework: Cl^-, SO_4^{2-}, ClO_4^-, and $RCOO^-$ (R = H, CH_3, C_2H_5). The simulations provide a microscopic mechanism for the reactions: they are found to be S_N2-type reactions, in which the TS is a strongly coupled ion pair $(NO_2^+NO_3^-)$ in substantial interaction with at least one water molecule. No evidence was found in the simulation for a mechanism that involves the nitronium ion as an independent reagent that attacks the anion.

The S_N2 reactions discussed in this paper could give the wrong impression that the overall kinetics of N_2O_5 in the presence of water should be first order in the concentration of the ion, and that the reactive uptake of N_2O_5 should be expected to depend strongly on the anion. Such a conclusion would however be misleading, and is indeed in contrast with the experiment, according to which the reactive uptake coefficient does not depend much on the concentration of the anion.[21,69] However, the model systems studied here address only the reactions in moderately sized clusters $(N_2O_5)(X)(H_2O)_{12}$. These are elementary reactions that are expected to correctly describe the microscopic dynamics, but not the macroscopic kinetics. The full macroscopic kinetics involves other processes, from diffusion to hydrolysis, and these alter the dependence upon concentration. Treatment of these processes lies outside the scope of this paper, and the model used is inadequate for these properties.

The simulations suggest a molecular level interpretation for the recent experiment by Staudt et al.,[47] in which formation of $ClNO_2$ from the reaction of N_2O_5 with 0.5 M NaCl was found to be suppressed by the presence of sulfate and acetate ions in the solution. According to the present results, this is likely to be because of the efficient reactivities of sulfate and acetate ions that compete with $ClNO_2$-forming reaction of Cl^- to form the reaction intermediates $SO_4NO_2^-$ and $HCOONO_2$. The cluster experiments using mass-spectrometric methods may

https://dx.doi.org/10.1021/acs.jpca.9b09095
J. Phys. Chem. A 2020, 124, 711−720

offer possibilities to observe these new intermediate species predicted by simulations.

We conclude by mentioning that systems of 12 water molecules are already quite computationally demanding to calculate with DFT. Thus, an increase in system size to model more realistic surfaces becomes impractical at this level of theory. We propose to study larger clusters in the future, but with a less computationally demanding level of theory. Already obtained results suggest an increased role for theoretical simulations, integrated with experiments, of the chemistry atmospheric aerosol particles.

■ AUTHOR INFORMATION

Corresponding Author

R. Benny Gerber − *Department of Chemistry, University of California, Irvine, Irvine 92697, California, United States; Institute of Chemistry and Fritz Haber Research Center, Hebrew University of Jerusalem, Jerusalem 91904, Israel;* orcid.org/0000-0001-8468-0258; Phone: +972-2-6585732; Email: benny@fh.huji.ac.il

Other Authors

Natalia V. Karimova − *Department of Chemistry, University of California, Irvine, Irvine 92697, California, United States;* orcid.org/0000-0002-4616-1884

James Chen − *Department of Chemistry, University of California, Irvine, Irvine 92697, California, United States*

Joseph R. Gord − *Department of Chemistry, University of Wisconsin-Madison, Madison 53706, Wisconsin, United States;* orcid.org/0000-0002-7235-6693

Sean Staudt − *Department of Chemistry, University of Wisconsin-Madison, Madison 53706, Wisconsin, United States;* orcid.org/0000-0002-3535-1260

Timothy H. Bertram − *Department of Chemistry, University of Wisconsin-Madison, Madison 53706, Wisconsin, United States;* orcid.org/0000-0002-3026-7588

Gilbert M. Nathanson − *Department of Chemistry, University of Wisconsin-Madison, Madison 53706, Wisconsin, United States;* orcid.org/0000-0002-6921-6841

Complete contact information is available at: https://pubs.acs.org/10.1021/acs.jpca.9b09095

Notes

The authors declare no competing financial interest.

Additional data related to this paper can be accessed from the NSF-CAICE Data Repository (doi: 10.6075/J0RN367K) or may be requested from the authors.

■ ACKNOWLEDGMENTS

This research was supported by NSF through the NSF Center for Aerosol Impacts on Chemistry of the Environment (NSF-CAICE), CHE-1801971. The authors thank Dr. Laura McCaslin and Dr. B. Hirshberg for discussions. Additionally, this work used the Extreme Science and Engineering Discovery Environment (XSEDE),[70] which is supported by grant number TG-CHE170064.

■ REFERENCES

(1) Finlayson-Pitts, B. J.; Pitts, J. N., Jr. *Chemistry of the Upper and Lower Atmosphere*; Elsevier, 2000.

(2) Zhong, J.; Kumar, M.; Anglada, J. M.; Martins-Costa, M. T. C.; Ruiz-Lopez, M. F.; Zeng, X. C.; Francisco, J. S. Atmospheric Spectroscopy and Photochemistry at Environmental Water Interfaces. *Annu. Rev. Phys. Chem.* **2019**, *70*, 45−69.

(3) Griffith, E. C.; Perkins, R. J.; Telesford, D.-M.; Adams, E. M.; Cwiklik, L.; Allen, H. C.; Roeselová, M.; Vaida, V. Interaction of l-Phenylalanine with a Phospholipid Monolayer at the Water-Air Interface. *J. Phys. Chem. B* **2015**, *119*, 9038−9048.

(4) Chang, W. L.; Bhave, P. V.; Brown, S. S.; Riemer, N.; Stutz, J.; Dabdub, D. Heterogeneous Atmospheric Chemistry, Ambient Measurements, and Model Calculations of N_2O_5: A Review. *Aerosol Sci. Technol.* **2011**, *45*, 665−695.

(5) Evans, M. J. Impact of New Laboratory Studies of N_2O_5 Hydrolysis on Global Model Budgets of Tropospheric Nitrogen Oxides, Ozone, and OH. *Geophys. Res. Lett.* **2005**, *32*, L09813−4.

(6) Macintyre, H. L.; Evans, M. J. Sensitivity of a Global Model to the Uptake of N_2O_5 by Tropospheric Aerosol. *Atmos. Chem. Phys.* **2010**, *10*, 7409−7414.

(7) Brown, S. S.; Dubé, W. P.; Fuchs, H.; Ryerson, T. B.; Wollny, A. G.; Brock, C. A.; Bahreini, R.; Middlebrook, A. M.; Neuman, J. A.; Atlas, E.; et al. Reactive Uptake Coefficients for N_2O_5 Determined from Aircraft Measurements during the Second Texas Air Quality Study: Comparison to Current Model Parameterizations. *J. Geophys. Res.* **2009**, *114*, D00F10.

(8) Thornton, J. A.; Abbatt, J. P. D. N_2O_5 Reaction on Submicron Sea Salt Aerosol: Kinetics, Products, and the Effect of Surface Active Organics. *J. Phys. Chem. A* **2005**, *109*, 10004−10012.

(9) Brown, S. S.; Stutz, J. Nighttime Radical Observations and Chemistry. *Chem. Soc. Rev.* **2012**, *41*, 6405−6447.

(10) Karimova, N. V.; McCaslin, L. M.; Gerber, R. B. Ion Reactions in Atmospherically-Relevant Clusters: Mechanisms, Dynamics and Spectroscopic Signatures. *Faraday Discuss.* **2019**, *217*, 342−360.

(11) Ahern, A. T.; Goldberger, L.; Jahl, L.; Thornton, J.; Sullivan, R. C. Production of N_2O_5 and $ClNO_2$ through Nocturnal Processing of Biomass-Burning Aerosol. *Environ. Sci. Technol.* **2018**, *52*, 550−559.

(12) Martins-Costa, M. T. C.; Anglada, J. M.; Francisco, J. S.; Ruiz-Lopez, M. Theoretical Investigation of the Photoexcited NO_2+H_2O Reaction at the Air-Water Interface and Its Atmospheric Implications. *Chem.—Eur. J.* **2019**, *25*, 13899−13904.

(13) Mozurkewich, M.; Calvert, J. G. Reaction Probability of N_2O_5 on Aqueous Aerosols. *J. Geophys. Res.* **1988**, *93*, 15889−15896.

(14) Riemer, N. Impact of the Heterogeneous Hydrolysis of N_2O_5 on Chemistry and Nitrate Aerosol Formation in the Lower Troposphere under Photosmog Conditions. *J. Geophys. Res.* **2003**, *108*, 4144.

(15) Hoffman, R. C.; Gebel, M. E.; Fox, B. S.; Finlayson-Pitts, B. J. Knudsen Cell Studies of the Reactions of N2O5 and ClONO2 with NaCl: Development and Application of a Model for Estimating Available Surface Areas and Corrected Uptake Coefficients. *Phys. Chem. Chem. Phys.* **2003**, *5*, 1780−1789.

(16) Finlayson-Pitts, B. J.; Ezell, M. J.; Pitts, J. N. Formation of Chemically Active Chlorine Compounds by Reactions of Atmospheric NaCl Particles with Gaseous N2O5 and ClONO2. *Nature* **1989**, *337*, 241−244.

(17) Thornton, J. A.; Kercher, J. P.; Riedel, T. P.; Wagner, N. L.; Cozic, J.; Holloway, J. S.; Dubé, W. P.; Wolfe, G. M.; Quinn, P. K.; Middlebrook, A. M.; et al. A Large Atomic Chlorine Source Inferred from Mid-Continental Reactive Nitrogen Chemistry. *Nature* **2010**, *464*, 271−274.

(18) Morris, E. D.; Niki, H. Reaction of Dinitrogen Pentoxide with Water. *J. Phys. Chem.* **1973**, *77*, 1929−1932.

(19) Dentener, F. J.; Crutzen, P. J. Reaction of N_2O_5 on Tropospheric Aerosols: Impact on the Global Distributions of NO_x, O_3, and OH. *J. Geophys. Res.: Atmos.* **1993**, *98*, 7149−7163.

(20) Hanway, D.; Tao, F.-M. A Density Functional Theory and Ab Initio Study of the Hydrolysis of Dinitrogen Pentoxide. *Chem. Phys. Lett.* **1998**, *285*, 459−466.

(21) Gaston, C. J.; Thornton, J. A. Reacto-Diffusive Length of N_2O_5 in Aqueous Sulfate- and Chloride-Containing Aerosol Particles. *J. Phys. Chem. A* **2016**, *120*, 1039−1045.

(22) Hirshberg, B.; Rossich Molina, E.; Götz, A. W.; Hammerich, A. D.; Nathanson, G. M.; Bertram, T. H.; Johnson, M. A.; Gerber, R. B. N_2O_5 at Water Surfaces: Binding Forces, Charge Separation, Energy Accommodation and Atmospheric Implications. *Phys. Chem. Chem. Phys.* **2018**, *20*, 17961−17976.
(23) Mentel, T. F.; Sohn, M.; Wahner, A. Nitrate Effect in the Heterogeneous Hydrolysis of Dinitrogen Pentoxide on Aqueous Aerosols. *Phys. Chem. Chem. Phys.* **1999**, *1*, 5451−5457.
(24) McNamara, J. P.; Hillier, I. H. Structure and Reactivity of Dinitrogen Pentoxide in Small Water Clusters Studied by Electronic Structure Calculations. *J. Phys. Chem. A* **2000**, *104*, 5307−5319.
(25) Hammerich, A. D.; Finlayson-Pitts, B. J.; Gerber, R. B. Mechanism for Formation of Atmospheric Cl Atom Precursors in the Reaction of Dinitrogen Oxides with HCl/Cl^- on Aqueous Films. *Phys. Chem. Chem. Phys.* **2015**, *17*, 19360−19370.
(26) Bertram, T. H.; Thornton, J. A. Toward a General Parameterization of N_2O_5 Reactivity on Aqueous Particles: The Competing Effects of Particle Liquid Water, Nitrate and Chloride. *Atmos. Chem. Phys.* **2009**, *9*, 8351−8363.
(27) Simon, H.; Kimura, Y.; McGaughey, G.; Allen, D. T.; Brown, S. S.; Coffman, D.; Dibb, J.; Osthoff, H. D.; Quinn, P.; Roberts, J. M. Modeling Heterogeneous ClNO2 Formation, Chloride Availability, and Chlorine Cycling in Southeast Texas. *Atmos. Environ.* **2010**, *44*, 5476−5488.
(28) Kercher, J. P.; Riedel, T. P.; Thornton, J. A. Chlorine Activation by N_2O_5: Simultaneous, in Situ Detection of $ClNO_2$ and N_2O_5 by Chemical Ionization Mass Spectrometry. *Atmos. Meas. Tech.* **2009**, *2*, 193−204.
(29) Sun, Y.; Zhang, Q.; Wang, W. Adsorption and Heterogeneous Reactions of $ClONO_2$ and N_2O_5 on/with NaCl Aerosol. *RSC Adv.* **2016**, *6*, 46336−46344.
(30) Sarwar, G.; Simon, H.; Xing, J.; Mathur, R. Importance of Tropospheric $ClNO_2$ Chemistry across the Northern Hemisphere. *Geophys. Res. Lett.* **2014**, *41*, 4050−4058.
(31) Roberts, J. M.; Osthoff, H. D.; Brown, S. S.; Ravishankara, A. R.; Coffman, D.; Quinn, P.; Bates, T. Laboratory Studies of Products of N_2O_5 Uptake on Cl^- Containing Substrates. *Geophys. Res. Lett.* **2009**, *36*, L20808−5.
(32) Shaloski, M. A.; Gord, J. R.; Staudt, S.; Quinn, S. L.; Bertram, T. H.; Nathanson, G. M. Reactions of N_2O_5 with Salty and Surfactant-Coated Glycerol: Interfacial Conversion of Br^- to Br_2 Mediated by Alkylammonium Cations. *J. Phys. Chem. A* **2017**, *121*, 3708−3719.
(33) Phillips, G. J.; Thieser, J.; Tang, M.; Sobanski, N.; Schuster, G.; Fachinger, J.; Drewnick, F.; Borrmann, S.; Bingemer, H.; Lelieveld, J.; et al. Estimating N_2O_5; Uptake Coefficients Using Ambient Measurements of NO_3, N_2O_5, $ClNO_2$ and Particle-Phase Nitrate. *Atmos. Chem. Phys.* **2016**, *16*, 13231−13249.
(34) Behnke, W.; George, C.; Scheer, V.; Zetzsch, C. Production and Decay of $ClNO_2$ from the Reaction of Gaseous N_2O_5 with NaCl Solution: Bulk and Aerosol Experiments. *J. Geophys. Res.: Atmos.* **1997**, *102*, 3795−3804.
(35) Platt, U. F.; Winer, A. M.; Biermann, H. W.; Atkinson, R.; Pitts, J. N. Measurement of Nitrate Radical Concentrations in Continental Air. *Environ. Sci. Technol.* **1984**, *18*, 365−369.
(36) Bertram, T. H.; Thornton, J. A.; Riedel, T. P.; Middlebrook, A. M.; Bahreini, R.; Bates, T. S.; Quinn, P. K.; Coffman, D. J. Direct Observations of N_2O_5 Reactivity on Ambient Aerosol Particles. *Geophys. Res. Lett.* **2009**, *36*, L19803.
(37) Armstrong, D. A.; Huie, R. E.; Lymar, S.; Koppenol, W. H.; Merényi, G.; Neta, P.; Stanbury, D. M.; Steenken, S.; Wardman, P. Standard Electrode Potentials Involving Radicals in Aqueous Solution: Inorganic Radicals. *Bioinorg. React. Mech.* **2013**, *9*, 59.
(38) Kelleher, P. J.; Menges, F. S.; DePalma, J. W.; Denton, J. K.; Johnson, M. A.; Weddle, G. H.; Hirshberg, B.; Gerber, R. B. Trapping and Structural Characterization of the $XNO_2 \cdot NO_3^-$ (X = Cl, Br, I) Exit Channel Complexes in the Water-Mediated $X^- + N_2O_5$ Reactions with Cryogenic Vibrational Spectroscopy. *J. Phys. Chem. Lett.* **2017**, *8*, 4710−4715.
(39) McCaslin, L. M.; Johnson, M. A.; Gerber, R. B. Mechanisms and Competition of Halide Substitution and Hydrolysis in Reactions of N_2O_5 with Seawater. *Sci. Adv.* **2019**, *5*, No. eaav6503.
(40) McNamara, J. P.; Hillier, I. H. Exploration of the Atmospheric Reactivity of N_2O_5 and HCl in Small Water Clusters Using Electronic Structure Methods. *Phys. Chem. Chem. Phys.* **2000**, *2*, 2503−2509.
(41) Thornton, J. A.; Kercher, J. P.; Riedel, T. P.; Wagner, N. L.; Cozic, J.; Holloway, J. S.; Dubé, W. P.; Wolfe, G. M.; Quinn, P. K.; Middlebrook, A. M.; et al. A Large Atomic Chlorine Source Inferred from Mid-Continental Reactive Nitrogen Chemistry. *Nature* **2010**, *464*, 271−274.
(42) Riedel, T. P.; Wagner, N. L.; Dubé, W. P.; Middlebrook, A. M.; Young, C. J.; Öztürk, F.; Bahreini, R.; VandenBoer, T. C.; Wolfe, D. E.; Williams, E. J.; et al. Chlorine Activation within Urban or Power Plant Plumes: Vertically Resolved $ClNO_2$ and Cl_2 Measurements from a Tall Tower in a Polluted Continental Setting: Chlorine Activation within Plumes. *J. Geophys. Res.: Atmos.* **2013**, *118*, 8702−8715.
(43) McDuffie, E. E.; Fibiger, D. L.; Dubé, W. P.; Lopez Hilfiker, F.; Lee, B. H.; Jaeglé, L.; Guo, H.; Weber, R. J.; Reeves, J. M.; Weinheimer, A. J.; et al. $ClNO_2$ Yields From Aircraft Measurements During the 2015 Winter Campaign and Critical Evaluation of the Current Parameterization. *J. Geophys. Res.: Atmos.* **2018**, *123*, 12994−13015.
(44) Tham, Y. J.; Wang, Z.; Li, Q.; Wang, W.; Wang, X.; Lu, K.; Ma, N.; Yan, C.; Kecorius, S.; Wiedensohler, A.; et al. Heterogeneous N_2O_5 Uptake Coefficient and Production Yield of $ClNO_2$ in Polluted Northern China: Roles of Aerosol Water Content and Chemical Composition. *Atmos. Chem. Phys.* **2018**, *18*, 13155.
(45) Wagner, N. L.; Riedel, T. P.; Young, C. J.; Bahreini, R.; Brock, C. A.; Dubé, W. P.; Kim, S.; Middlebrook, A. M.; Öztürk, F.; Roberts, J. M.; et al. N_2O_5 Uptake Coefficients and Nocturnal NO_2 Removal Rates Determined from Ambient Wintertime Measurements: Wintertime N_2O_5 Uptake Coefficients. *J. Geophys. Res.: Atmos.* **2013**, *118*, 9331−9350.
(46) Riedel, T. P.; Bertram, T. H.; Crisp, T. A.; Williams, E. J.; Lerner, B. M.; Vlasenko, A.; Li, S.-M.; Gilman, J.; de Gouw, J.; Bon, D. M.; et al. Nitryl Chloride and Molecular Chlorine in the Coastal Marine Boundary Layer. *Environ. Sci. Technol.* **2012**, *46*, 10463−10470.
(47) Staudt, S.; Gord, J. R.; Karimova, N. V.; McDuffie, E. E.; Brown, S. S.; Gerber, R. B.; Nathanson, G. M.; Bertram, T. H. Sulfate and Carboxylate Suppress the Formation of $ClNO_2$ at Atmospheric Interfaces. *ACS Earth Space Chem.* **2019**, *3*, 1987−1997.
(48) Meng, Z.; Seinfeld, J. H.; Saxena, P. Gas/Aerosol Distribution of Formic and Acetic Acids. *Aerosol Sci. Technol.* **1995**, *23*, 561−578.
(49) Hey, J. C.; Doyle, E. J.; Chen, Y.; Johnston, R. L. Isomers and Energy Landscapes of Micro-Hydrated Sulfite and Chlorate Clusters. *Philos. Trans.: Math., Phys. Eng. Sci.* **2018**, *376*, 20170154.
(50) Hey, J. C.; Smeeton, L. C.; Oakley, M. T.; Johnston, R. L. Isomers and Energy Landscapes of Perchlorate-Water Clusters and a Comparison to Pure Water and Sulfate-Water Clusters. *J. Phys. Chem. A* **2016**, *120*, 4008−4015.
(51) Smeeton, L. C.; Farrell, J. D.; Oakley, M. T.; Wales, D. J.; Johnston, R. L. Structures and Energy Landscapes of Hydrated Sulfate Clusters. *J. Chem. Theory Comput.* **2015**, *11*, 2377−2384.
(52) Martínez, L.; Andrade, R.; Birgin, E. G.; Martínez, J. M. PACKMOL: A Package for Building Initial Configurations for Molecular Dynamics Simulations. *J. Comput. Chem.* **2009**, *30*, 2157−2164.
(53) Adamo, C.; Barone, V. Toward Reliable Density Functional Methods without Adjustable Parameters: The PBE0 Model. *J. Chem. Phys.* **1999**, *110*, 6158−6170.
(54) Shao, Y.; Gan, Z.; Epifanovsky, E.; Gilbert, A. T. B.; Wormit, M.; Kussmann, J.; Lange, A. W.; Behn, A.; Deng, J.; Feng, X.; et al. Advances in Molecular Quantum Chemistry Contained in the Q-Chem 4 Program Package. *Mol. Phys.* **2015**, *113*, 184−215.
(55) Schmidt, M. W.; Baldridge, K. K.; Boatz, J. A.; Elbert, S. T.; Gordon, M. S.; Jensen, J. H.; Koseki, S.; Matsunaga, N.; Nguyen, K.

A.; Su, S.; et al. General Atomic and Molecular Electronic Structure System. *J. Comput. Chem.* **1993**, *14*, 1347−1363.
(56) Gillan, M. J.; Alfè, D.; Michaelides, A. Perspective: How Good Is DFT for Water? *J. Chem. Phys.* **2016**, *144*, 130901.
(57) Riera, M.; Götz, A. W.; Paesani, F. The I-TTM Model for Ab Initio-Based Ion−Water Interaction Potentials. II. Alkali Metal Ion−Water Potential Energy Functions. *Phys. Chem. Chem. Phys.* **2016**, *18*, 30334−30343.
(58) Grimme, S. Semiempirical GGA-Type Density Functional Constructed with a Long-Range Dispersion Correction. *J. Comput. Chem.* **2006**, *27*, 1787−1799.
(59) Gonzalez, C.; Schlegel, H. B. Reaction Path Following in Mass-Weighted Internal Coordinates. *J. Phys. Chem.* **1990**, *94*, 5523−5527.
(60) Glendening, E. D.; Landis, C. R.; Weinhold, F. *NBO 6.0*: Natural Bond Orbital Analysis Program. *J. Comput. Chem.* **2013**, *34*, 1429−1437.
(61) Marx, D.; Hutter, J. *Ab Initio Molecular Dynamics: Basic Theory and Advanced Methods*; Cambridge University Press: Cambridge; New York, 2009.
(62) Gerber, R. B.; Shemesh, D.; Varner, M. E.; Kalinowski, J.; Hirshberg, B. Ab Initio and Semi-Empirical Molecular Dynamics Simulations of Chemical Reactions in Isolated Molecules and in Clusters. *Phys. Chem. Chem. Phys.* **2014**, *16*, 9760−9775.
(63) Hirshberg, B.; Gerber, R. B. Formation of Carbonic Acid in Impact of CO_2 on Ice and Water. *J. Phys. Chem. Lett.* **2016**, *7*, 2905−2909.
(64) Thornton, J. A.; Braban, C. F.; Abbatt, J. P. D. N_2O_5 Hydrolysis on Sub-Micron Organic Aerosols: The Effect of Relative Humidity, Particle Phase, and Particle Size. *Phys. Chem. Chem. Phys.* **2003**, *5*, 4593.
(65) Thornton, J. A.; Abbatt, J. P. D. N_2O_5 Reaction on Submicron Sea Salt Aerosol: Kinetics, Products, and the Effect of Surface Active Organics. *J. Phys. Chem. A* **2005**, *109*, 10004−10012.
(66) Raff, J. D.; Njegic, B.; Chang, W. L.; Gordon, M. S.; Dabdub, D.; Gerber, R. B.; Finlayson-Pitts, B. J. Chlorine Activation Indoors and Outdoors via Surface-Mediated Reactions of Nitrogen Oxides with Hydrogen Chloride. *Proc. Natl. Acad. Sci. U.S.A.* **2009**, *106*, 13647−13654.
(67) Ishikawa, Y.; Binning, R. C. Ab Initio Direct Molecular Dynamics Studies of Atmospheric Reactions: Interconversion of Nitronium Ion and Nitric Acid in Small Water Clusters. *Computational Chemistry: Reviews of Current Trends*; World Scientific, 2002; Vol. 7, pp 187−244.
(68) Relph, R. A.; Guasco, T. L.; Elliott, B. M.; Kamrath, M. Z.; McCoy, A. B.; Steele, R. P.; Schofield, D. P.; Jordan, K. D.; Viggiano, A. A.; Ferguson, E. E.; et al. How the Shape of an H-Bonded Network Controls Proton-Coupled Water Activation in HONO Formation. *Science* **2010**, *327*, 308−312.
(69) Van Doren, J. M.; Watson, L. R.; Davidovits, P.; Worsnop, D. R.; Zahniser, M. S.; Kolb, C. E. Temperature Dependence of the Uptake Coefficients of Nitric Acid, Hydrochloric Acid and Nitrogen Oxide (N_2O_5) by Water Droplets. *J. Phys. Chem.* **1990**, *94*, 3265−3269.
(70) Towns, J.; Cockerill, T.; Dahan, M.; Foster, I.; Gaither, K.; Grimshaw, A.; Hazlewood, V.; Lathrop, S.; Lifka, D.; Peterson, G. D.; et al. XSEDE: Accelerating Scientific Discovery. *Comput. Sci. Eng.* **2014**, *16*, 62−74.

https://dx.doi.org/10.1021/acs.jpca.9b09095
J. Phys. Chem. A 2020, 124, 711−720